

Effects of various intake valve timings and spark timings on combustion, cyclic THC and NO_x emissions during cold start phase with idle operation in CVVT engine[†]

Kwanhee Choi, Hyungmin Lee, In Goo Hwang, Cha-Lee Myung and Simsoo Park^{*}

School of Mechanical Engineering, Korea University 1, 5-Ga, Anam-dong, Seongbuk-gu, Seoul 136-701, Korea

(Manuscript Received January 9, 2008; Revised May 26, 2008; Accepted June 13, 2008)

Abstract

In a gasoline SI engine, valve events and spark timings put forth a major influence on overall efficiency, fuel economy, and exhaust emissions. Residual gases controlled by the valve overlap can be used to reduce NO_x emissions and the spark retardation technique can be used to improve raw THC emissions and catalyst light-off performance during the cold start phase. This paper investigated the behaviors of the engine and its combustion characteristics with various intake valve timings and spark timings during the fast idle condition and cold start. And cyclic THC and NO_x emissions were measured at the exhaust port and their formation mechanisms were examined with fast response gas analyzers. As a result, THCs and NO_x were reduced by 35% and 23% with optimizing valve overlap and spark advance during the cold transient start phase. Consequently, the valve events and ignition timings were found to significantly affect combustion phenomena and cold-start emissions.

Keywords: CVVT; Valve overlap; Spark retardation; Fast response gas analyzer; Cold transient start

1. Introduction

During the last several years, the automobile industry has focused on the development of environmentally friendly vehicles to meet the reinforced emission legislation. More than 95% of total hydrocarbon (THC) emissions in Federal Test Procedure (FTP)-75 mode test were exhausted within the first few cycles before catalyst activation in super ultra low emission vehicle (SULEV). Therefore, various factors of engine combustion, aftertreatment and engine control have been investigated for cold start emission reduction [1, 2]. Technologies for reducing cold start emissions are exhaust aftertreatment systems, such as thin wall catalysts, electrically heated catalysts (EHC),

flow optimized exhaust manifolds, and stainless steel exhaust manifolds, which have proven to be quite effective to meet the future emission regulations [3].

In addition to aftertreatment technologies, spark timing retard is considered as a very effective technique for reducing THC emissions. As spark timing at cold start is retarded from minimum spark advance for best torque (MBT), exhaust gas temperature increases, and hence it remarkably reduces the THC emissions at phase 1 of the FTP-75 mode. When spark timing is aggressively retarded, engine torque is decreased and combustion stability (such as cyclic indicated mean effective pressure (IMEP) variation) deteriorates. To improve the combustion stability, research on advanced engine concepts such as variable valve timing and lift electronic control (VTEC) or swirl control valve (SCV) for high-turbulence in-cylinder flow engines has been conducted to achieve a large amount of spark timing retard [4].

Also, a continuously variable valve timing (CVVT)

[†] This paper was recommended for publication in revised form by Associate Editor Kyoung Doug Min

^{*} Corresponding author. Tel.: +82 2 3290 3368, Fax.: +82 2 926 9290

E-mail address: spark@korea.ac.kr

© KSME & Springer 2008

system has been widely adopted since it can enhance the engine performance, reduce exhaust emissions and fuel consumption, simultaneously. With the CVVT system of the intake cam phaser, maximum torque and power are improved through the optimization of valve timing according to the overall engine operation condition [5, 6]. Intake valve timing influences the providing of internal exhaust gas recirculation (EGR), which reduces the emissions of nitro-oxide (NO_x) and fuel consumption with the longer valve overlap period at part load. In conventional CVVT engines, valve overlap used to be eliminated to improve the startability and stable idling quality at the start phase. However, some amounts of overlap promote fuel atomization by the blow-back gases which are at high temperature [7].

In this study, combustion phenomena according to various intake valve timings and spark timings were evaluated to achieve low cold-start emissions and rapid catalyst light-off performance during the cold start phase including the idle transient operation of the gasoline CVVT engine. Also, time-resolved THC and NO_x were measured at the exhaust port with high resolution gas analyzers to investigate the characteristics of their formation and reduction mechanisms.

2. Experimental apparatus and method

An in-line 4, 1,998cc gasoline engine with 16 valves was used in the experiment. The engine has a CVVT system which controls the intake valve timing continuously. The CVVT system is a ‘cam-phasing type’ with a fixed valve duration; therefore, when the intake valve opening (IVO) timing is advanced or retarded, the closing timing is simultaneously changed. Table 1 shows the detailed specifications of the test engine.

Table 1. Specifications of test engine.

	Specifications
Engine Type	In-line, DOHC 16 V
Bore (mm)	86.0
Stroke (mm)	86.0
Displacement (cc)	1,998
Valve timing	Intake : Variable Exhaust : 34 / 10
Valve Duration (°CA)	Intake : 236 Exhaust : 224
Compression Ratio	10.5 : 1

To determine behaviors of the engine and the exhaust gases during a fast idle condition after a cold start, the temperature of the cooling water was maintained at 25°C with 1400 rpm, idle and $\lambda=1.0$. Intake valve timings were changed from BTDC 10° (with 20° valve overlap) to ATDC 10° (without valve overlap) by 10 degrees and spark timings from BTDC 20° to ATDC 5°. Cylinder pressure traces were measured at the 4th cylinder with spark-plug type pressure sensor and the signals from the sensor were resolved by the combustion analyzer. The schematic diagram of the experimental apparatus is shown in Fig. 1.

2.1 Fast response gas analyzer

Cyclic THC and NO_x emission characteristics were acquired at the exhaust port by using FR-FID (Fast Response Flame Ionization Detector) and FR-CLD (Fast Response Chemiluminescent Detector) by Cambustion Ltd. Sampling points were 15 mm away from the exhaust valves of the 3rd and the 4th exhaust ports, respectively.

The analysis mechanisms of the fast response gas analyzer are as follows. Hydrocarbon components produce ions in a hydrogen-air flame. FR-FID uses the characteristic that the rate of ionization is proportional to the concentration of HCs in the exhaust sample gases. The response time of the FR-FID is under 1 ms because of the shorter distance between the sampling probe and detector than that of the conventional THC analyzer [8]. FR-CLD uses the light emission from the reaction between the NO molecules and the ozone. This light emission is exactly proportional to the concentration of NO in a sample flow. This light intensity is measured at the main control unit by a photo-multiplier to detect the NO concentration [9]. The response time of the FR-CLD is about 4 ms, a resolution that can detect the cycle-

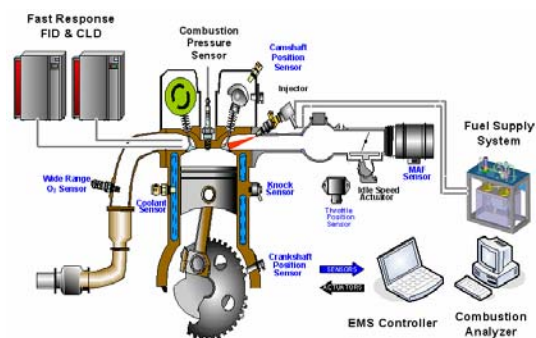


Fig. 1. Schematic diagram of experimental apparatus.

by-cycle emission formation in an internal combustion engine.

2.2 Engine control logic

The main advantage of spark timing retard from MBT is the faster catalyst activation than that of the conventional spark timing operation. As the spark timing is retarded, the unburned fuel is oxidized during the exhaust stroke at the exhaust valves and exhaust ports, so the engine-out THC emissions can be greatly reduced. In addition, the exhaust temperature and catalyst bed temperature rise faster than those of the MBT spark timing. However, spark timing retard results in loss of power and unstable engine operation. To compensate for increasing engine roughness, air quantity through the throttle should be increased to adjust the target engine speed and decrease the cyclic variations of the engine. Furthermore, power loss results in a loss of fuel economy. However, because the adoption of spark timing retard is activated for a very short interval at cold start, fuel economy loss is negligible.

3. Experimental results and discussion

3.1 Steady operation result

3.1.1 Engine operation characteristic

Fig. 2 shows the intake manifold pressure for various intake valve openings and spark timings at 1400 rpm, idle, and $\lambda=1.0$. When the intake valve opens earlier, manifold pressure increases by the residual gases, which are at high temperature and pressure. And the intake manifold pressure also increases as the

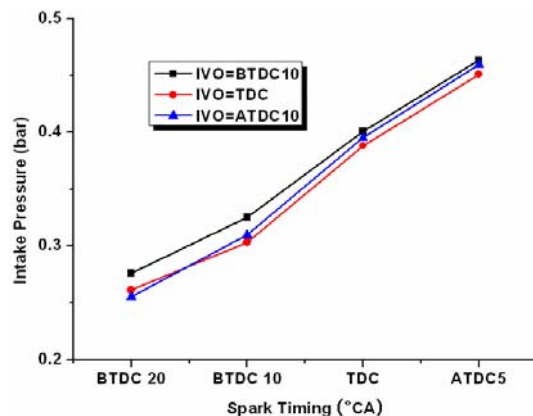


Fig. 2. Intake manifold pressure (1400 rpm/idle, $\lambda=1.0$, 25°C coolant temp).

spark timing is retarded, because of the increment in the throttle position to maintain the target engine speed. As a result, when the spark timing was retarded from BTDC 20° to ATDC 5°, the intake pressure rose about 1.7 times from 264mbar to 458 mbar.

Fig. 3 represents the exhaust gas and catalyst bed temperature with respect to spark timings. Compared with the results of the spark timing of BTDC 20°, the exhaust gas and catalyst temperatures of ATDC 5° increased about 121°C and 172°C, respectively. However, intake openings did not affect the exhaust gas temperature, so the spark timing was considered to be more effective on the reduction of HC emissions during the first stage of the start condition.

Figs. 4 and 5 show the stabilities of the engine indicated by the cyclic variations of IMEP. Advanced intake opening induces more backflow to the intake port, makes combustion quality inferior as shown in Fig. 4. Also, a retardation of spark showed a similar trend because of the decrease in the expansion work and combustion speed as shown in Fig. 5. Therefore, when advanced intake openings and retarded spark timings are applied, additional flow strengthening devices such as SCV and IACV (Intake Air Control

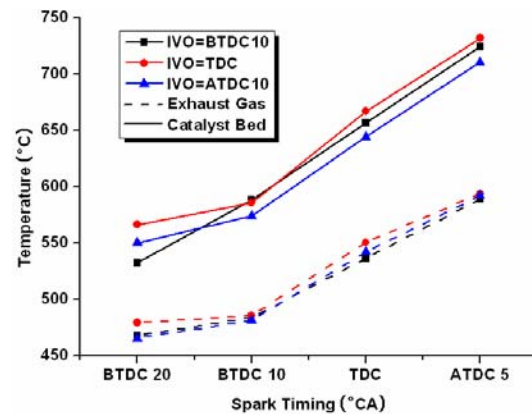


Fig. 3. Exhaust gas and catalyst bed temperature (1400 rpm/idle, $\lambda=1.0$, 25°C coolant temp).

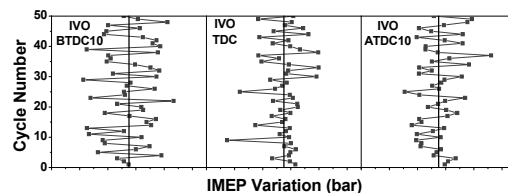


Fig. 4. Cyclic variation of IMEP with respect to intake opening (S/A=BTDC 10°, 1400 rpm/idle, $\lambda=1.0$, 25°C coolant temp).

Valve) should be considered.

3.1.2 Combustion analysis

Fig. 6 indicates the cylinder pressure with various intake openings. For the earlier intake timings, air charge in the cylinder was increased because of the higher pressure of the intake chamber. As a result, the peak pressure rose 1.0 bar at the IVO of BTDC 10° than that of ATDC 10°.

Cylinder pressure traces with various spark timings are shown in Fig. 7. The peak pressure for the spark timing of BTDC 20° was 5.4 bar, while that of ATDC 5° was 8.9 bar. Even if the peak pressures were relatively high for excessive spark timing retarded cases (TDC-ATDC 5°), the pressure profiles became smoother and broader during the expansion stroke than those of the normal spark timing cases (BTDC 20°-BTDC 10°), which means the combustion initiated during the early expansion stroke and lasted until

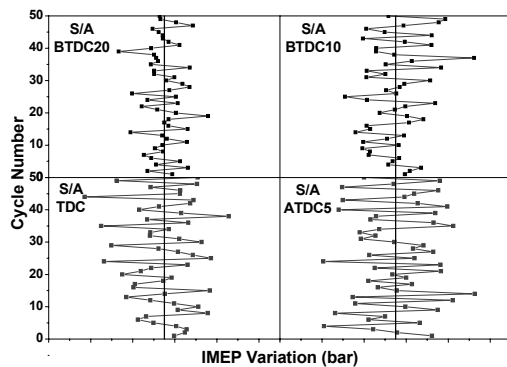


Fig. 5. Cyclic variation of IMEP with respect to spark timing (IVO=ATDC 10°, 1400rpm/idle, $\lambda=1.0$, 25°C coolant temp).

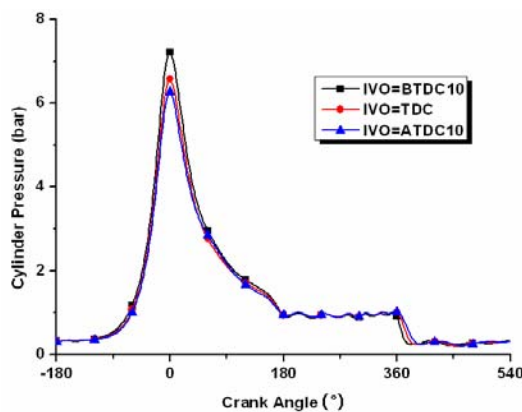


Fig. 6. Cylinder pressure with respect to intake openings (S/A = BTDC 10°, 1400 rpm/idle, $\lambda=1.0$, 25°C coolant temp).

the exhaust stroke. High cylinder pressure output with retarded spark timings (TDC and ATDC 5°) means that much air is required to maintain the target engine speed.

The location of maximum pressure occurred at TDC despite the change in spark timings because the pressure rise due to the combustion was much smaller than that of the compression of the air-fuel mixture by the piston movement. Therefore, to determine the effects of combustion on the cylinder pressure according to spark timings, the portion of the total pressure rise due to adiabatic compression was subtracted from the cylinder pressure. Eq. (1) represents the pressure difference calculated from volume change (Δp_v). Eq. (2) shows the relations of the pressure rise due to combustion (Δp_c), the actual cylinder pressure change (Δp) by experiment, and Δp_v [10]. The maxi-

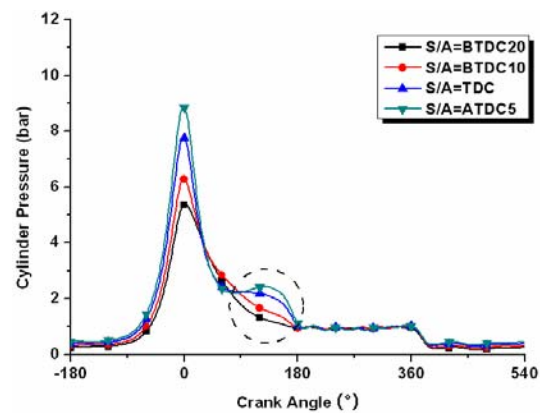


Fig. 7. Cylinder pressure with respect to spark timing (IVO = ATDC 10°, 1400 rpm/idle, $\lambda=1.0$, 25°C coolant temp).

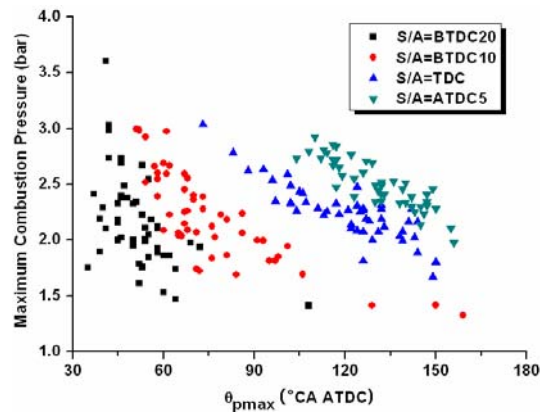


Fig. 8. Maximum combustion pressure $p_{c,max}$ and location of $p_{c,max}$ with respect to spark timing (IVO = ATDC 10°, 1400 rpm/idle, $\lambda=1.0$, 25°C coolant temp).

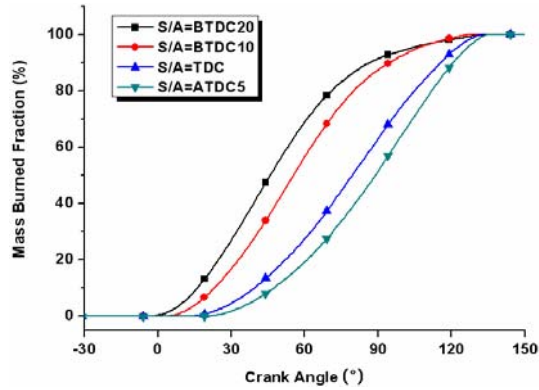


Fig. 9. Mass burned fraction with respect to spark timing (IVO = ATDC 10°, 1400 rpm/idle, $\lambda=1.0$, 25°C coolant temp).

imum values and locations for 50 cycles are represented in Fig. 8.

$$\Delta p_v = p_j - p_i = p_i \left[\left(\frac{V_i}{V_j} \right)^n - 1 \right] \quad (1)$$

$$\Delta p_c = \Delta p - \Delta p_v \quad (2)$$

As the ignition was retarded from BTDC 20° to ATDC 5°, the location of the maximum combustion pressure was delayed from ATDC 49° to ATDC 134° by an average of 50 cycles for each case.

Fig. 9 shows the combustion duration expressed as the fuel mass burned rate. As mentioned above, spark retard lowers flame propagation speed and extends the combustion process to the expansion stroke or even to the exhaust stroke. As a result, the crank angle of 50% fuel mass burned was located at ATDC 89° for the spark timing of ATDC 5° which was delayed about 43° in comparison with the result of BTDC 20° spark advance. Also, a combustion period from 10% to 90% of the fuel mass burned was extended about 3° in crank angle.

3.1.3 Cyclic THC and NOx emission characteristics

For early intake openings, some amount of unburned and burned gas flows backward into intake port from combustion chamber during the valve overlap. This reverse flow goes through the combustion process again with the fresh air-fuel mixture, which leads to the reoxidation of the unburned gases [11]. As a result, accumulated unburned hydrocarbon emission during one cycle was reduced by 7.7% for the IVO of BTDC 10° than that of ATDC 10° as shown

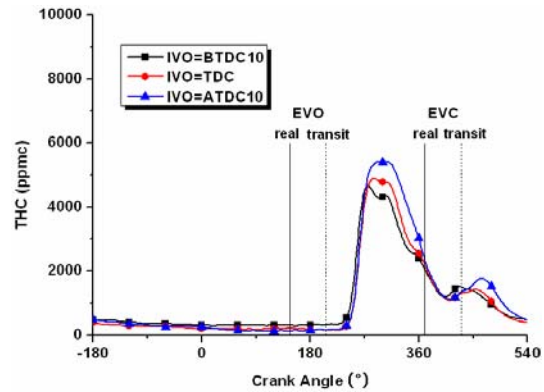


Fig. 10. Cycle resolved THC emission characteristic with respect to intake opening (S/A = BTDC 10°, 1400 rpm/idle, $\lambda=1.0$, 25°C coolant temp.)

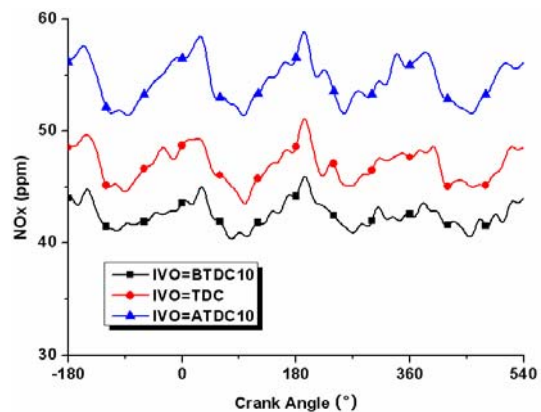


Fig. 11. Cycle resolved NOx emission characteristic with respect to intake opening (S/A = BTDC 10°, 1400 rpm/idle, $\lambda=1.0$, 25°C coolant temp).

in Fig. 10.

Early intake valve opening allows the burned gases to flow back into the low pressure intake port for a longer period of time because of the pressure gradient of the cylinder and intake system. Thus, the residual gases in the manifold are recirculated into the cylinder in the subsequent cycle leading to the reduction of NOx emissions with a low flame temperature. Therefore, cycle averaged NOx was decreased by about 22% with 20° extended valve overlap as shown in Fig. 11. Particularly, NOx traces showed four peaks during one cycle whereas THCs showed just one peak at the exhaust stroke. NOx chemistry, once formed during the combustion process, does not deoxidize like the HCs. So, the effect of the other cylinders is considered as the cause of the four peaks in the NOx traces [12].

Spark retardation is effective to the reduction of engine-out HC emission as well as improvement of the catalyst light-off performance. Accumulated unburned hydrocarbons reached the level of 1000 kppmc with BTDC 20° of spark advance and decreased by 66% to 340 kppmc with TDC of ignition as illustrated in Fig. 12. But when the spark timing was retarded aggressively to ATDC, a partial burn increased the amount of HCs to about 500 kppmc due to the deterioration of the combustion quality. Therefore, engine instability according to the ignition delay would need to be considered to maximize its benefit for reduction of the engine-out HCs.

Generally, NOx level with the retarded spark timing decreases due to the lower temperature in the combustion chamber. However, in this experiment, the mass air flow supplied into the cylinder was increased to maintain the target engine speed. As a re-

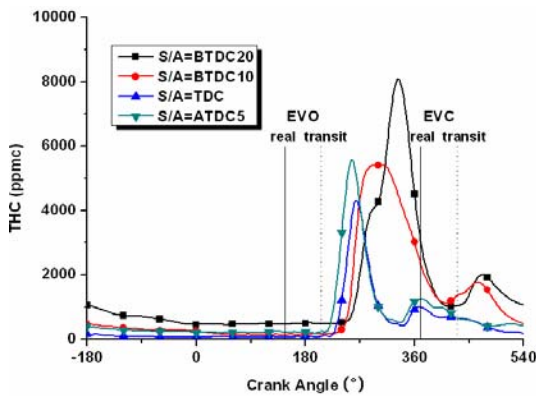


Fig. 12. Cycle resolved THC emission characteristic with respect to spark timing (IVO = ATDC 10°, 1400 rpm/idle, λ=1.0, 25°C coolant temp).

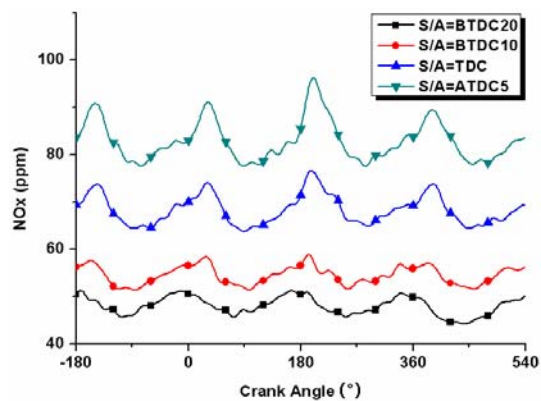


Fig. 13. Cycle resolved NOx emission characteristic with respect to spark timing (IVO = ATDC 10°, 1400rpm/idle, λ=1.0, 25°C coolant temp).

sult, the cylinder temperature and pressure increased with the spark retard. Therefore, these increases resulted in high amounts of NOx level, as shown in Fig. 13.

Comparing the spark at ATDC 5° with BTDC 20°, the average NOx values were nearly doubled from 48 ppm to 83 ppm. Therefore, when the ignition was retarded for raw THC and catalyst activation time during cold start, the nitro-oxide emission should be prevented by countermeasures such as adjustment of the valve overlap or supplement of the external EGR.

3.2 Time resolved cold start analysis

Fig. 14 represents the cylinder and intake pressures, THC, and NOx emissions with fixed spark timing, and various intake timings during the first 4 sec of

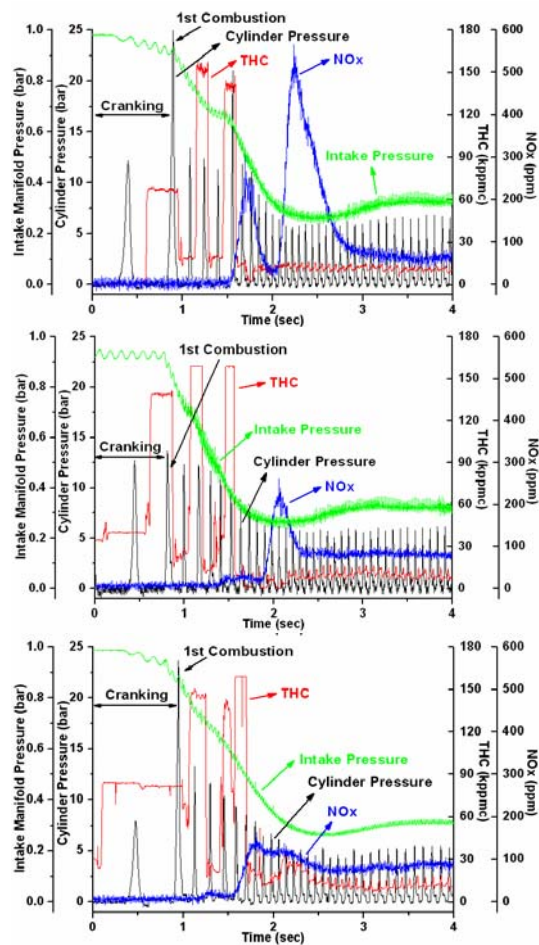


Fig. 14. Pressure, THC and NOx characteristics during 4 sec of cold start (S/A = BTDC 10°, λ=1.0 (at idle), 25°C coolant temp, IVO = BTDC 10°, TDC, ATDC 10° from above).

cold start.

Classifying the start phase of the engine into two stages, (a start stage from the first firing to 2 seconds and an idle stage after 2 seconds), the accumulated hydrocarbons in first stage were 155 kppmc at ATDC 10° of valve opening and 75 kppmc at BTDC 10°, which was a reduction of more than 50% with the increase of valve overlap 0 to 20°. The maximum NOx emission was increased by more than 3.5 times, from 163 ppm to 566 ppm, because the valve overlap enhanced the vaporization of fuel by hot backflow of the residuals. It promoted stable combustion during the start stage, with reduced THC and increased NOx. In the idle stage, THCs were at a level of 10 kppmc regardless of the intake valve timings and the NOx decreased from 84 ppm to 65 ppm with the increased valve overlap.

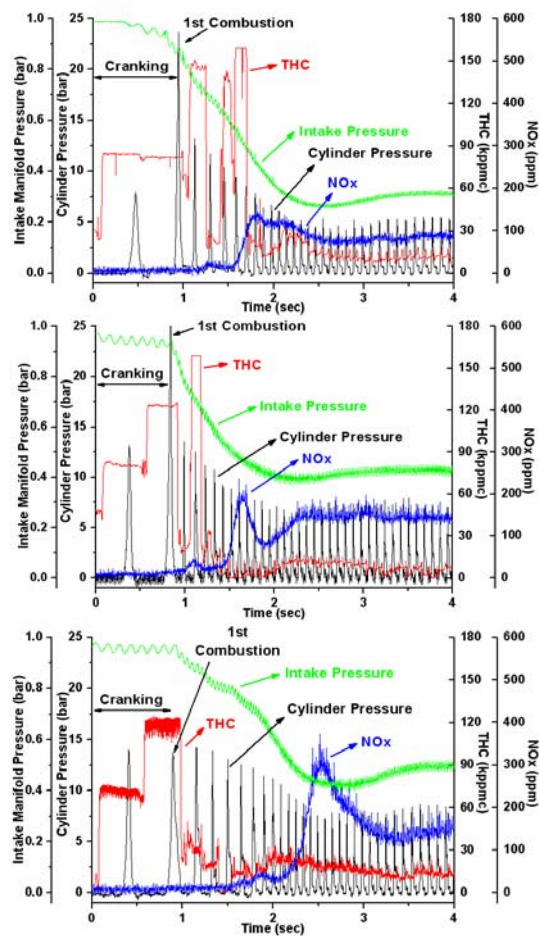


Fig. 15. Pressure, THC and NOx characteristics during 4 sec of cold start (IVO = ATDC 10°, $\lambda=1.0$ (at idle), 25°C coolant temp., S/A = BTDC 10°, TDC, ATDC 5° from above).

Fig. 15 indicates the cylinder and intake pressure, cyclic THC and NOx emissions with fixed valve timing and various spark timings during the first 4 seconds of cold start. With the spark retardation to ATDC 5°, the accumulated THC was measured to be 102 kppmc, which was 65% reduction from BTDC 10° spark advance, and that resulted in 155 kppmc. The maximum NOx value was measured to be 374ppm with ATDC 5° of spark advance, which was 2 times more than that with BTDC 10°. At the stable idle stage, NOx concentrations were about 84 ppm on average at BTDC 10° of ignition and 154 ppm at ATDC 5°. With the spark at TDC, exhausted hydrocarbons were about half level of that at BTDC 10°. However, THCs at ATDC 5° were almost the same level with that at BTDC 10° by the instabilities of the engine.

The catalyst light-off performance by spark retardation was determined by temperature traces of the catalyst bed with various ignition timings as shown in Fig. 16. The catalyst activation temperature was assumed as 250°C; it took 31 seconds to light-off the catalyst with BTDC 10° of spark advance, 23 seconds with TDC and 19 seconds with ATDC 5°, which was faster by 8 seconds and 12 seconds, respectively. This results show that ignition retardation logic has a positive effect on the enhancement of the catalyst performance as well as on the decrease of the engine-out hydrocarbons.

4. Conclusions

An investigation for reducing emissions during a cold start of a CVVT engine and analysis for combustion phenomena, cyclic THC and NOx emissions

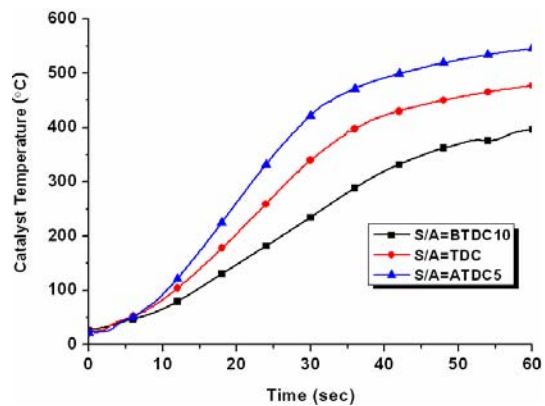


Fig. 16. Catalyst temperature during 60 sec after cold start (IVO = ATDC 10°, $\lambda=1.0$).

during fast idle and cold start were accomplished. The results are summarized as follows.

(1) Combustion stabilities and flame speeds were decreased with the advancement of the intake openings to BTDC 10° from ATDC 10° due to the backflow during the overlap. But it had a positive effect on the pumping loss due to high pressure residuals flowing to the intake port. Especially, the engine-out THC emissions were reduced 7.7% by re-burning of the residual gases, and NOx emission was reduced 22% because of lowered flame temperature.

(2) The temperatures of exhaust gases and catalyst bed were increased by about 120°C and 170°C, respectively, with spark retard to ATDC 5° from BTDC 20° because of the oxidation of unburned hydrocarbons at the exhaust port and catalyst. Therefore, high conversion efficiency can be obtained quickly by shortening the catalyst light-off time.

(3) The engine-out THCs were reduced by about 66% with ignition retard because of the subsequent oxidation of unburned fuels at the exhaust ports and the catalyst. However, ignition retard causes the combustion to be incomplete until the end of the expansion stroke, so expansion work decreases. Also, spark retard had negative effects on combustion such as lowered flame speed and deteriorated combustion stability. In particular, 73% more NOx was generated, because of the supplementary air to maintain the target engine speed. Therefore the intake valve timings and engine combustion characteristics should be considered when determining the amount of spark retardation.

(4) During cold start, valve overlap had positive effects on the vaporization of the fuel droplets due to the backflow of residual gases which is at high temperature. As a result, THCs were decreased to a level of 50%, and the maximum NOx was exhausted by more than 3.5 times. But the penalty in NOx at the start stage was not significant because the NOx shows minimum level in the idle stage with lower flame temperature due to the residuals. Therefore, the valve overlap has advantages in reducing cold-start THC and NOx emissions before catalyst activation.

(5) THCs were decreased to a level of 65% by retarding spark timing. Also, catalyst light-off time was shortened 12 seconds, so spark retardation was highly effective in reducing cold-start emissions. However, aggressive retardation to ATDC caused more THCs because combustion stability was aggravated; therefore charge motion control equipment should be

adopted such as a swirl and tumble device. Finally, NOx should be controlled with the IVO timing because the additional air supply results in high NOx emissions.

Acknowledgments

This study was funded by BK21 and the Ministry of Commerce, Industry and Energy.

References

- [1] C. E. Roberts and R. H. Stanglmaier, Investigation of intake timing effects on the cold start behavior of a spark ignition engine, *SAE Paper* No.1999-01-3622 (1999).
- [2] H. Santoso and W. K. Cheng, Mixture preparation and hydrocarbon emissions behaviors in the first cycle of SI engine cranking, *SAE Paper* No. 2002-01-2805 (2002).
- [3] F. Zhao, *Technologies for Near-Zero-Emission Gasoline-Powered Vehicles*, SAE international, Warrendale, USA, (2007).
- [4] H. Kwak, C. L. Myung and S. Park, Experimental investigation on the time resolved THC emission characteristics of liquid phase LPG injection (LPLi) engine during cold start, *Fuel* 86 (2007) 1475-1482.
- [5] G. B. Parvate-Patil, H. Hong and B. Gordon, An assessment of intake and exhaust philosophies for variable valve timing, *SAE Paper* No.2003-32-0078, *JSAE Paper* No.20034378 (2003).
- [6] H. B. Lee, H. Kwon and K. Min, Effects of various VVA systems on the engine fuel economy and optimization of a CVVT-VVL SI engine using 1D simulation, *Int. J. Automotive Technology* 8 (6) (2007) 675-685.
- [7] T. Kidokoro, K. Hoshi, K. Hikaru, K. Satoya, T. Watanabe, T. Fujiwara and H. Suzuki, Development of PZEV exhaust emission control system, *SAE Paper* No.2003-01-0817 (2003).
- [8] S. Schurov, T. Summers and N. Collings, Time resolved measurement of cold start HC concentration using the fast FID, *SAE Paper* No.961926 (1996).
- [9] M. Peckham, T. Hands, J. Burrell, N. Collings and S. Schurov, Real time in-cylinder and exhaust NO measurements in a production SI engine, *SAE Paper* No.980400 (1998).
- [10] J. B. Heywood, *International Combustion Engine Fundamentals*, McGraw-Hill, New York, USA

- (1988).
- [11] C. L. Myung, H. Kwak, I. G. Hwang and S. Park, Theoretical flow analysis and experimental study on time resolved THC formation with residual gas in a dual CVVT engine, *Int. J. Automotive Technology* 8 (6) (2007) 697-704.
- [12] J. M. Sung, H. W. Kim and K. H. Lee, Analysis on cycle-by-cycle NO emissions from an SI engine with fast NO analyzer, *Transaction of KSAE* 10 (2) (2002) 73-79.



Simsoo Park received his B.S. and M.S. degrees from Seoul National University in 1977 and 1979, respectively, and a Ph.D. from the State University of New York at Stony Brook. He served as a Principle Re-

search Engineer at Hyundai Motor Company, a Director for Publication of the KSME, a Technical Advisor of Hyundai-Kia Motor Company, and an Editing Director, Project Director, International Director, Accounting Director, and General Affair Director of KSAE. He is currently Vice President of Editing and International at KSAE and a professor of mechanical engineering at Korea University.